forum acusticum 2026
8-12 September · Graz, Austria

SYMMETRIC AND ASYMMETRIC EMBROIDERED MASS PATTERNS IN MEMBRANE VIBRATION MODES

Ahmed Mehrem[1], Luisa Euler[1], Tobias Hecht[1]

[1] *German Institutes of Textile and Fiber Research Denkendorf, Germany.*

This paper is a revised version of the authors' submitted manuscript that was peer-reviewed by at least two anonymous reviewers.

Abstract

This study investigates the transverse vibration of tensioned membranes with spatially periodic surface-mass variations that represent embroidered fabrics. A two-dimensional membrane model is discretized using finite differences with fixed boundary conditions. The resulting generalized eigenvalue problem accounts for heterogeneous surface mass density and is evaluated for four representative designs inspired by the common weave bindings plain, satin and twill, and an asymmetric layout. Computed natural frequencies and mode shapes are compared with the analytical solution for a uniform square membrane. Symmetric patterns largely preserve classical modal symmetry and near-degenerate mode pairs, whereas the asymmetric layout breaks symmetry, lifts degeneracy, and produces larger frequency shifts accompanied by distorted mode shapes.

Keywords: *tensioned membranes, textile acoustics, vibration modes, modal analysis, mass heterogeneity*

1. Introduction

Tensioned membranes are widely used in acoustics, lightweight structures, and textile systems, where their vibration characteristics influence sound radiation, damping, and structural response [1], [2]. Classical membrane theory describes transverse vibration using a two-dimensional wave equation under the assumptions of uniform in-plane tension and homogeneous surface mass density [3], [4].

In textile membranes, these assumptions are often violated. Embroidered fabrics inherently exhibit spatially periodic heterogeneity due to yarn interlacing and overlapping in the weave structure [5], [6] and locally added embroidery yarns, which lead to deterministic variations in surface mass density. Previous studies have largely focused on homogeneous membranes or have treated heterogeneity as a stochastic perturbation. In contrast, embroidery designs generate repeatable and well-defined patterns that can be intentionally selected and therefore treated as a design parameter rather than an imperfection [7].

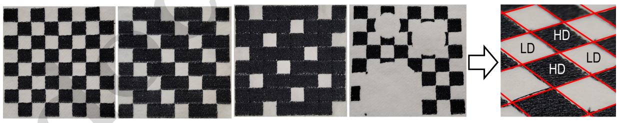

Figure 1: (Left) Surface mass density distributions for the studied emboidery designs, from left to right: plain weave, twill, satin and asymmetric (black yarn embroidered on white fabric); (Right) Illustration of high density (HD) and low density (LD) areas in the patterns.

In this work, we study tensioned membranes with embroidery as idealized surface-mass distributions using a finite difference formulation. The designs introduce varying levels of symmetry and anisotropy. Natural frequencies, mode shapes, and frequency-response functions are computed for four representative embroidery designs inspired by the common weave bindings plain weave, satin and twill, and an asymmetric layout. They are compared with the analytical solution for a uniform square membrane to isolate the roles of symmetry and mass contrast.

2. Model and Numerical Method

The transverse vibration of a thin membrane defined on a square domain $\Omega = [0, L]_x \times [0, L]_y$ and subjected to uniform in-plane tension T is governed by

$$\rho(x, y)\frac{\partial^2 u}{\partial t^2} = T\nabla^2 u, \tag{1}$$

where $u(x, y, t)$ denotes the transverse displacement and $\rho(x, y)$ is the spatially varying surface mass density ($\mathrm{kg/m^2}$). Assuming harmonic motion of the form $u(x, y, t) = \phi(x, y)e^{i\omega t}$ leads to the generalized eigenvalue problem

Corresponding author: *ahmed.mehrem@ditf.de.*

$$T\nabla^2\phi = \lambda\rho(x,y)\phi, \qquad \lambda = \omega^2, \tag{2}$$

where ω is the angular natural frequency and $f = \omega/(2\pi)$ the corresponding frequency in Hz. Homogeneous Dirichlet boundary conditions are imposed along the boundary,

$$\phi = 0 \quad \text{on } \partial\Omega. \tag{3}$$

The domain is discretized on a uniform Cartesian grid with spacing $\Delta x = \Delta y$, and the Laplacian is approximated using a standard five-point finite difference stencil. After removing boundary nodes, the discrete system is written in matrix form as

$$T\mathbf{L}\boldsymbol{\phi} = \lambda\mathbf{M}\boldsymbol{\phi}, \tag{4}$$

where $\mathbf{L}$ is the sparse Laplacian matrix and $\mathbf{M}$ is a diagonal mass matrix constructed from the discretized density field. The lowest eigenpairs are computed using MATLAB's `eigs` solver. For the special case of uniform density $\rho(x,y) = \rho_0$, the membrane has the classical analytical solution

$$\phi_{mn}(x,y) = \sin\left(\frac{m\pi x}{L}\right)\sin\left(\frac{n\pi y}{L}\right), \tag{5}$$

with corresponding natural frequencies

$$f_{mn} = \frac{1}{2}\sqrt{\frac{T}{\rho_0}}\sqrt{\left(\frac{m}{L}\right)^2 + \left(\frac{n}{L}\right)^2}, \tag{6}$$

where $m, n \in \mathbb{N}$. These analytical solutions provide the reference case for evaluating the effect of mass heterogeneity (Fig. 2).

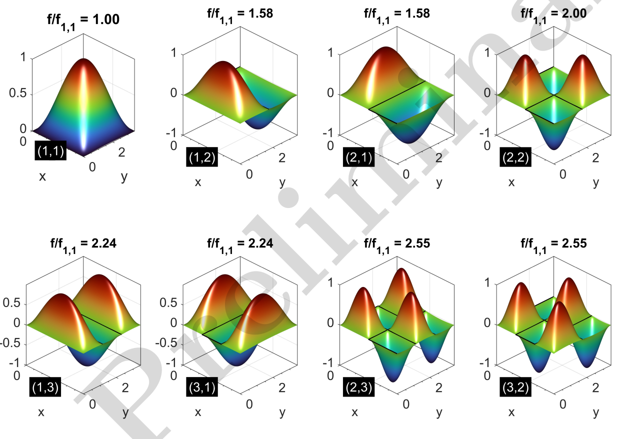

Figure 2: Analytical vibration modes of a square membrane with uniform density. Each subplot shows a normalized mode shape $\phi_{mn}(x,y)$ and corresponding natural frequency f_{mn}.

The embroidered membrane designs are modeled as piecewise-constant density fields with two surface-mass levels (light and heavy regions, i.e., without and with embroidery yarns). Four representative configurations are investigated, in the following referred to as plain weave, satin, twill, and an asymmetric layout (Fig. 1).

3. Results and Discussion

The influence of deterministic surface-mass heterogeneity is evaluated for the four chosen embroidery configurations on a woven substrate (plain weave, satin, twill, and asymmetric; Fig. 1).

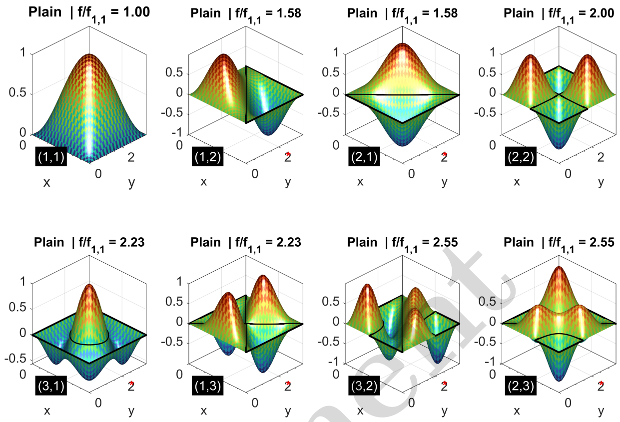

Figure 3: Normalized vibration mode shapes for the plain weave mass pattern. Each subplot shows a computed eigenmode $\phi(x,y)$ with the corresponding normalized frequency $f/f_{1,1}$ and mode index (m,n). A red asterisk marks modes with near-degenerate eigenfrequencies ($|\Delta f| < 0.05$ Hz).

Frequencies are reported in normalized form $f/f_{1,1}$, where $f_{1,1}$ denotes the fundamental frequency of each configuration. All patterned cases employ a two-level density field with $\rho_{\text{heavy}} = 0.8$ kg/m^2 and $\rho_{\text{light}} = 0.1$ kg/m^2 (8:1 contrast). Although each spectrum is normalized by its own fundamental frequency, higher modes remain sensitive to both the mean surface density and the spatial organization of the mass pattern.

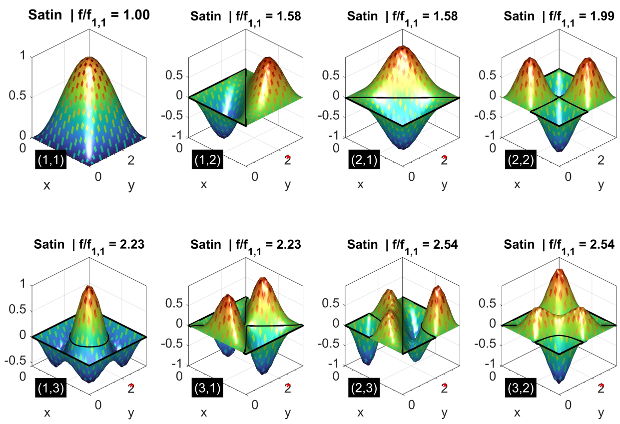

Figure 4: Normalized vibration mode shapes for the satin mass pattern. Each subplot shows a computed eigenmode $\phi(x,y)$ with the corresponding normalized frequency $f/f_{1,1}$ and mode index (m,n). A red asterisk marks modes with near-degenerate eigenfrequencies ($|\Delta f| < 0.05$ Hz).

Figures 3–6 show the computed eigenmodes. Across all configurations, the fundamental $(1,1)$ mode remains dominated by boundary conditions and retains a single central antinode. Pattern-dependent effects become increasingly visible at higher orders. For the symmetric layouts (plain, satin, and twill), the nodal topology remains close to that of the uniform membrane, and permutation mode pairs such as $(1, 2)$ and $(2, 1)$ or $(1, 3)$ and $(3, 1)$ remain nearly degenerate.

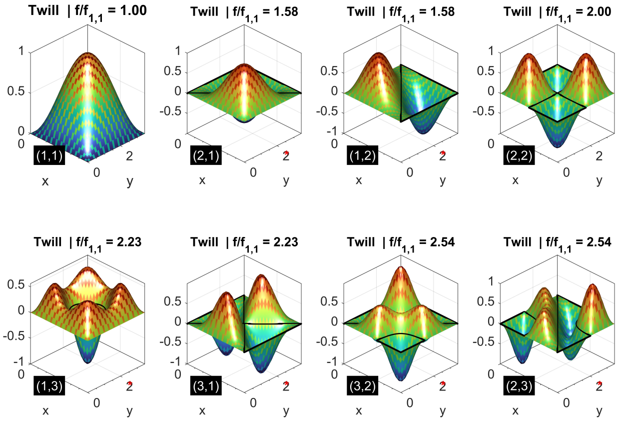

Figure 5: Normalized vibration mode shapes for the twill mass pattern. Each subplot shows a computed eigenmode $\phi(x, y)$ with the corresponding normalized frequency $f/f_{1,1}$ and mode index (m, n). A red asterisk marks modes with near-degenerate eigenfrequencies ($|\Delta f| < 0.05$ Hz).

In the plain weave pattern, the checkerboard mass distribution introduces a regular tile-scale modulation, while the lobes themselves remain smooth and symmetric. Twill behaves in a similar way, with smooth modal surfaces and no visible distortion of the lobe geometry. Satin, however, shows slightly more pronounced local variations within the lobes, where small surface irregularities appear, even though global symmetry and degeneracy are still maintained.

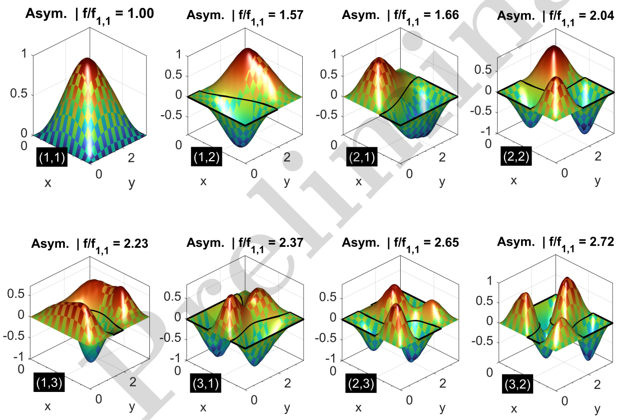

Figure 6: Normalized vibration mode shapes for the asymmetric mass pattern. Each subplot shows a computed eigenmode $\phi(x, y)$ with the corresponding normalized frequency $f/f_{1,1}$ and mode index (m, n).

In contrast, the asymmetric configuration breaks mirror symmetry and produces a clear lifting of degeneracy. Nodal lines become curved and uneven, and several modes display visible hybridization, indicating stronger coupling between nearby modal families.

These effects are reflected quantitatively in Fig. 7, where the satin configuration follows the analytical uniform-membrane trend most closely across all modes. The plain weave pattern exhibits larger downward shifts due to the strong checkerboard mass contrast, while twill introduces moderate but systematic deviations associated with its directional periodicity. The asymmetric layout shows the strongest departure from the analytical reference, accompanied by a clear lifting of modal degeneracy and progressive frequency redistribution.

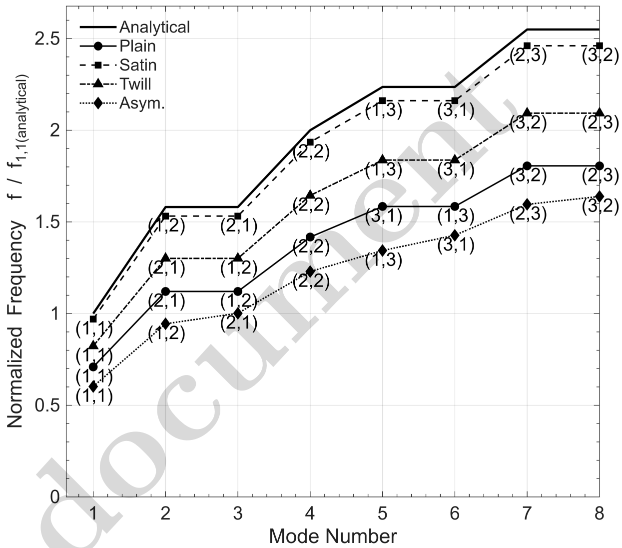

Figure 7: Comparison of computed natural frequencies for different weave patterns. The analytical reference corresponds to a uniform membrane. Labels indicate mode indices (m, n). Simulations were performed with a surface mass contrast of $\rho_{\text{heavy}} = 0.8$ and $\rho_{\text{light}} = 0.1$, corresponding to an 8:1 density ratio.

The steady-state frequency responses under central harmonic excitation are shown in Fig. 8. Resonance peaks coincide with the computed eigenfrequencies for all configurations. Satin exhibits pronounced and well-separated peaks across the first modes, indicating strong modal participation and preserved symmetry. Twill also produces sharp low-order resonances, although higher modes show slight redistribution of amplitude. In contrast, the plain pattern shows comparatively reduced higher-order peak amplitudes. The asymmetric configuration presents a dominant first resonance followed by strongly suppressed and irregular higher modes, reflecting symmetry breaking and reduced spatial alignment between the excitation region and modal antinodes.
The observed trends can be interpreted through two coupled mechanisms. First, the mean surface density influences the global inertial loading and shifts the frequency scale. Second, the spatial organization of heavy and light regions governs symmetry and directional bias, thereby controlling degeneracy preservation, modal distortion, and modal participation. Regular symmetric designs act as structured pertur-

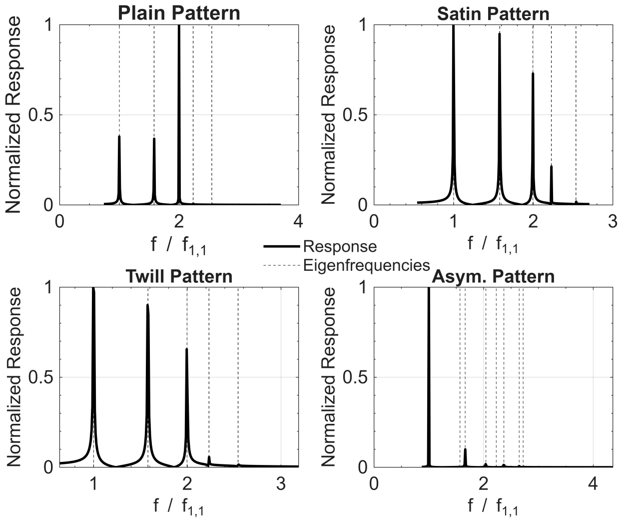

Figure 8: Frequency response curves under harmonic excitation for each pattern. Vertical dashed lines mark the simulated eigenfrequencies.

bations of the classical membrane problem, largely preserving nodal topology. In contrast, asymmetric layouts break spatial symmetry more strongly, leading to degeneracy lifting, hybridized mode shapes, and reduced higher-order resonance participation.

4. Conclusions

A numerical study of tensioned square membranes with surface-mass heterogeneity created by embroidery was presented. Comparison with the uniform-membrane reference shows that symmetric periodic layouts (plain weave, satin, and twill) largely preserve the classical modal families and near-degenerate permutation pairs, with moderate and structured frequency shifts without fundamentally changing the nodal topology. In contrast, the asymmetric layout breaks spatial symmetry, lifts degeneracy, and suppresses higher-order modal participation in the forced-response spectrum. The results demonstrate that both global mass scaling and spatial mass organization provide deterministic parameters for tuning membrane resonances.

References

[1] P. M. Morse and K. Ingard, *Theoretical Acoustics*. Princeton University Press, 1968.

[2] W. Soedel, *Vibrations of Shells and Plates*. Boca Raton, FL, USA: CRC Press, 2004.

[3] A. W. Leissa, *Vibration of Plates*. Washington D.C.: NASA SP-160, National Aeronautics and Space Administration, 1969.

[4] S. S. Rao, *Vibration of Continuous Systems*, 2nd ed. Hoboken, NJ, USA: John Wiley & Sons, 2017, ISBN: 9781119424147.

[5] A. Rawal, A. Majumdar, and V. Kumar, "Textile architecture for composite materials: Back to basics," *Oxford Open Materials Science*, vol. 3, no. 1, itad017, 2023.

[6] K. Gandhi, *Woven textiles: Principles, technologies and applications*. Woodhead Publishing, 2019.

[7] M. K. Ozturk, K. Kalinova, B. Nergis, and C. Candan, "Comparison of resonance frequency of a nanofibrous membrane and a homogeneous membrane structure," *Textile Research Journal*, vol. 83, no. 20, pp. 2204–2210, 2013.